Supplemental Information

Hematopoietic stem cell quiescence promotes error prone DNA repair and mutagenesis

Mary Mohrin, Emer Bourke, David Alexander, Matthew Warr, Keegan Barry-Holson, Michelle M. Le Beau, Ciaran Morrison and Emmanuelle Passegué.

INVENTORY OF SUPPLEMENTARY INFORMATION

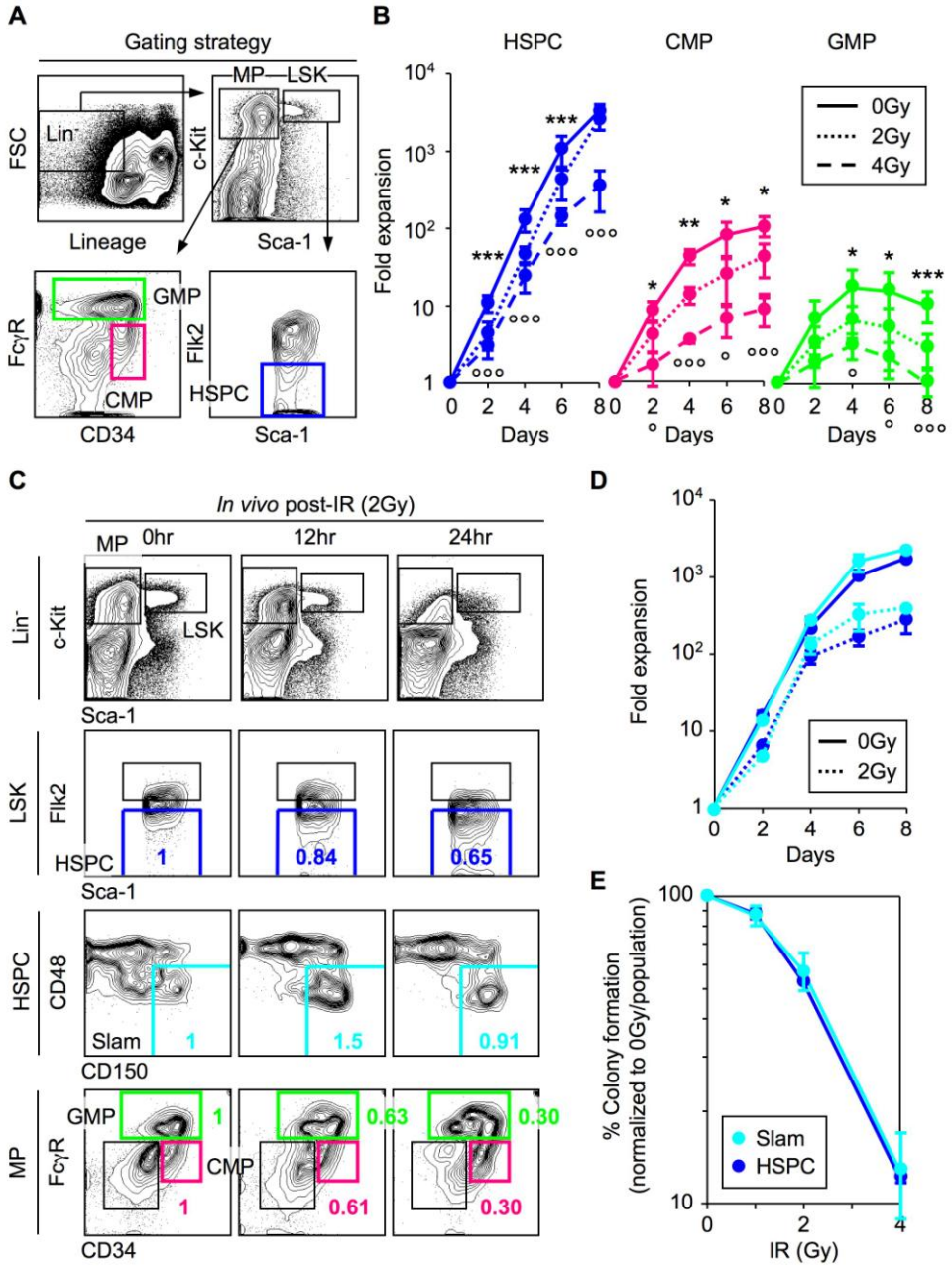

Figure S1, Effect of radiation on mouse hematopoietic stem cells and myeloid progenitors, related to Figure 1. A, Gating strategy used to isolate HSPCs, CMPs and GMPs from mouse bone marrow. **B**, Growth of unirradiated and irradiated HSPCs, CMPs and GMPs in liquid media (n = 5 to 9; ***p ≤ 0.001; **p ≤ 0.01; *p ≤ 0.05 [2Gy *vs*. 0Gy]; °°°p ≤ 0.001; °p ≤ 0.05 [4Gy *vs*. 2Gy]). **C**, *In vivo* effects of 2Gy irradiation. Mice were analyzed after 12h and 24h post-irradiation (IR) and compared to unirradiated mice (0h) for changes in the frequency of the indicated bone marrow populations analyzed by flow cytometry. The fold change is indicated for each population. **D**, Growth of irradiated Slam-HSCs and HSPCs in liquid media (n = 3). **E**, Clonogenic survival assay in methylcellulose comparing the radioresistance of the most immature Slam-HSC and HSPC (n = 3).

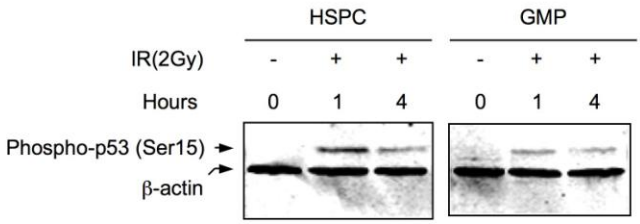

Figure S2, p53 activation levels in irradiated HSPCs and GMPs, related to Figure 2. Western blot analysis of phospho-p53 (Ser15) protein levels in unirradiated (0 hour) and 2Gy-irradiated HSPCs and GMPs 1 and 4 hours after exposure (proteins extracted from 70,000 isolated cells per lane; β-actin is used as loading control).

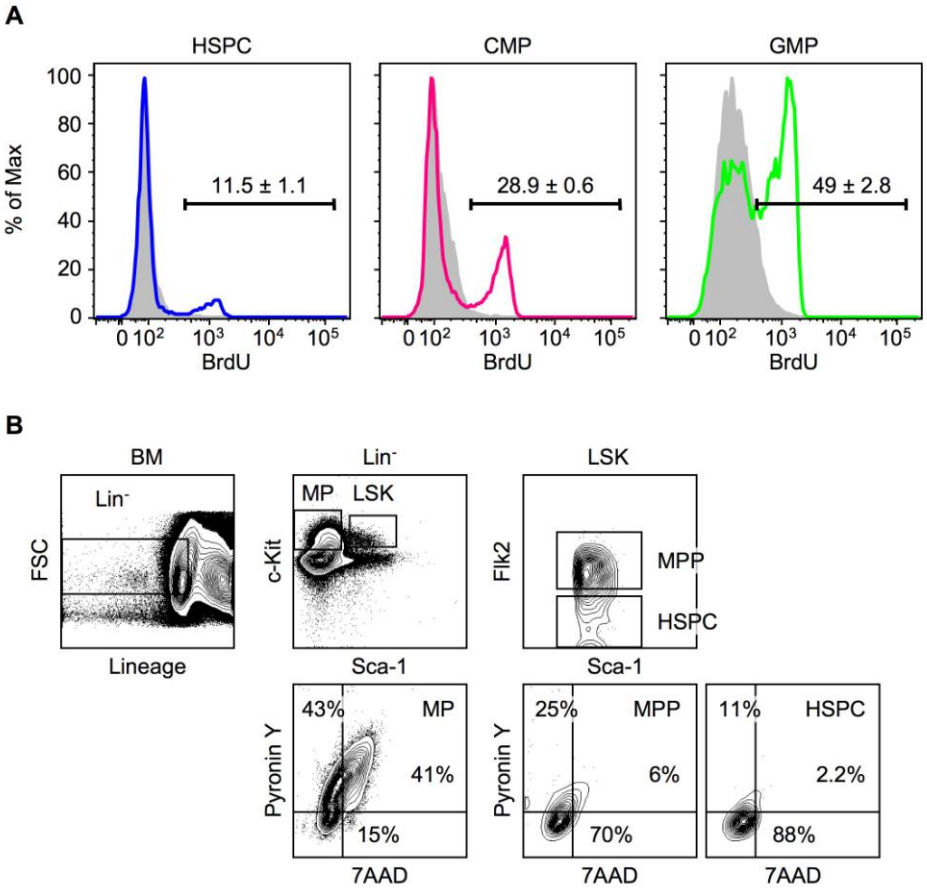

Figure S3, Proliferation and cells cycle status of HSPCs and MPs, related to Figure 4. A, Basal proliferation rates of unirradiated HSPCs (blue), CMPs (pink) and GMPs measured after 1 hour BrdU pulse *in vitro* (n = 3). The grey shapes represent BrdU staining on cells that have not been incubated with BrdU. **B**, Example of combined surface and intracellular 7AAD/Pyronin Y (PY) staining for analysis of cell cycle distribution in HSPCs, $Flk2^{+}$ LSK multipotent progenitors (MPP) and $Lin^{-}/Sca\text{-}1^{-}/c\text{-}kit^{+}$ MPs. Quiescent G_0 cells are $7AAD^{2n}/PY^{-}$ while proliferative G_1 and $S\text{-}G_2/M$ cells are $7AAD^{2n}/PY^{+}$ and $7AAD^{\geq 2n\text{-}4n}/PY^{+}$, respectively.

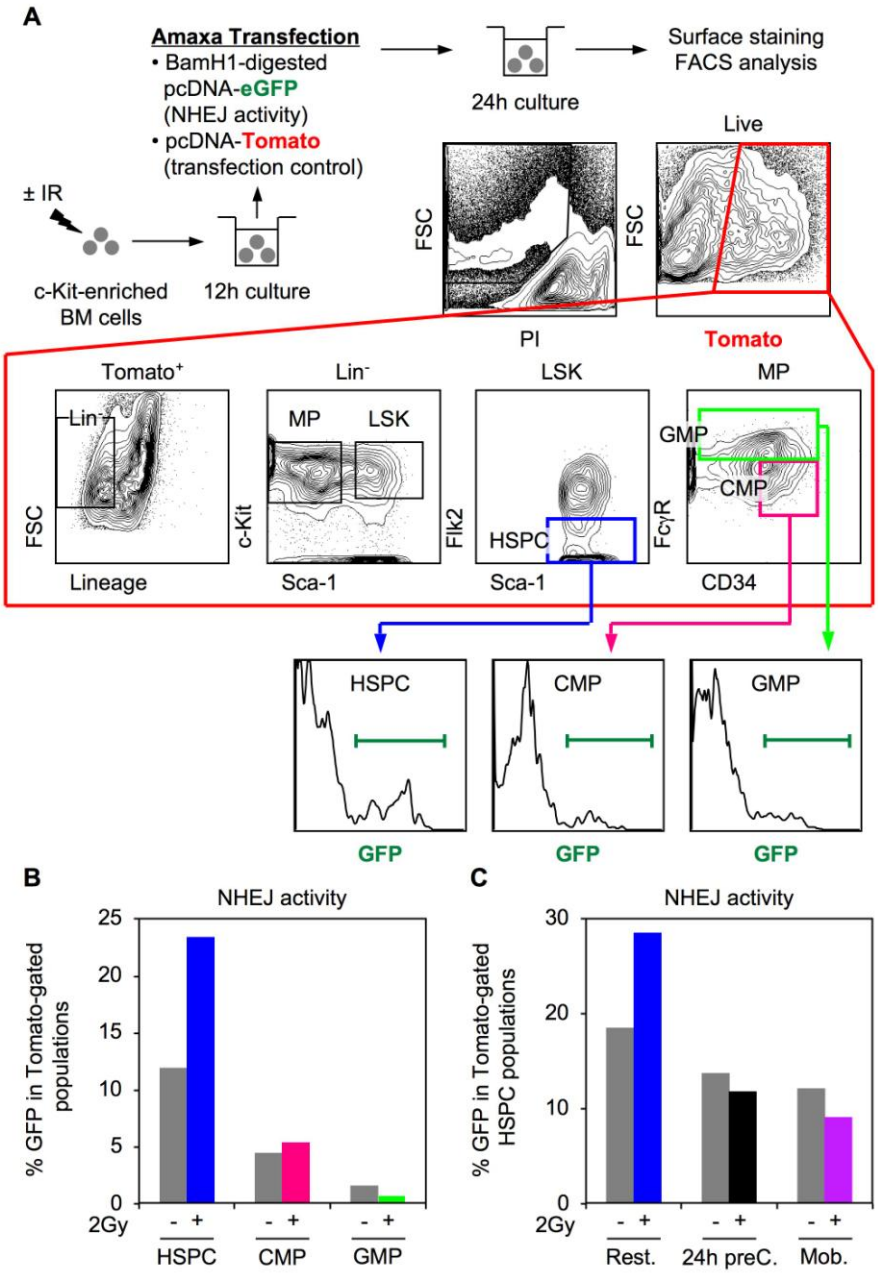

Figure S4, Assessment of NHEJ activity in HSPCs and MPs, related to Figure 4 and Figure 6. A, Experimental scheme of the NHEJ activity assay. **B**, Representative example of NHEJ activity in unirradiated (grey) or 2Gy-irradiated HSPCs (blue), CMPs (pink) and GMPs (green). Single measurement was performed for each condition. Fold changes upon IR-treatment were calculated as [% GFP in 2Gy-irradiated cells]/[% GFP in unirradiated cells]. **C**, Representative example of NHEJ activity in unirradiated (grey) or 2Gy-irradiated (color) resting (blue) and proliferating (24h preC, black; Mob., purple) HSPCs.

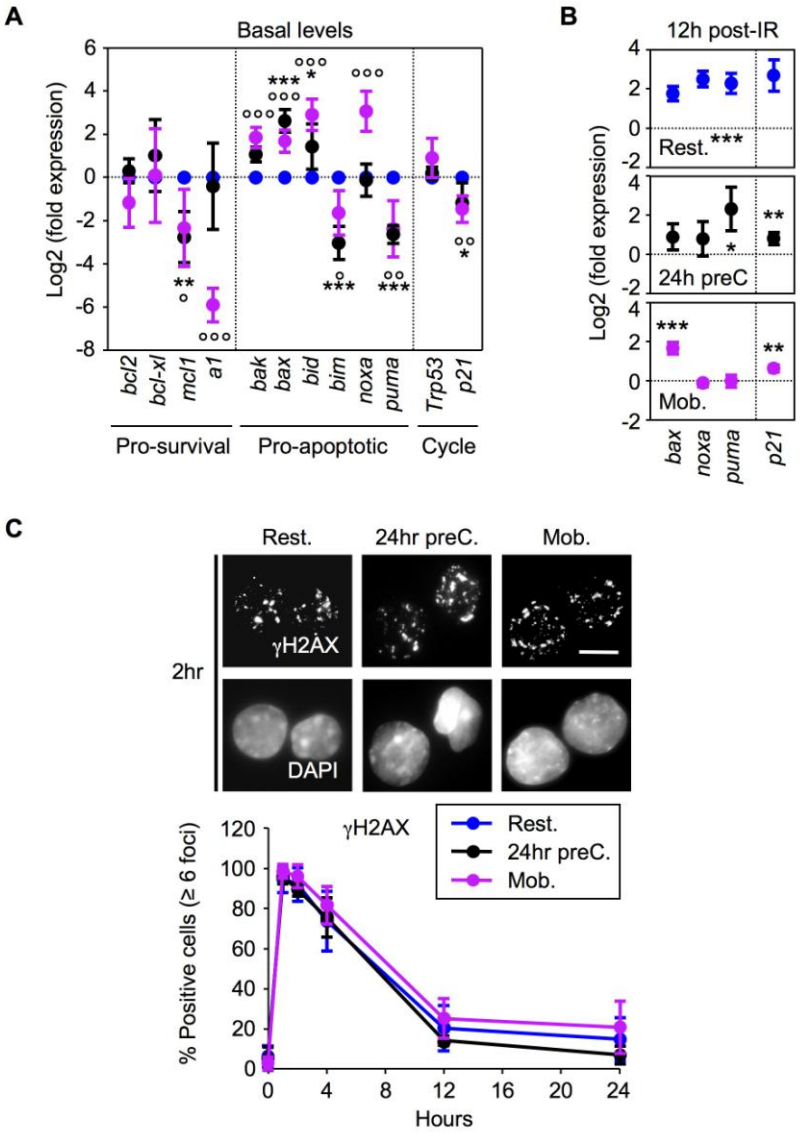

Figure S5, Increased basal apoptosis in proliferating HSPCs, related to Figure 5 and Figure 6. A, QRT-PCR analysis of basal levels in resting and proliferating HSPCs. Results are expressed as log2 fold expression compared to levels measured in resting HSPCs (n = 3; ***p ≤ 0.001, **p ≤ 0.01, *p ≤ 0.05 [24h preC *vs*. Rest. HSPCs]; °°°p ≤ 0.001, °°p ≤ 0.01, °p ≤ 0.05 [Mob. *vs*. Rest. HSPCs]). **B**, QRT-PCR analysis of p53-target genes in resting (Fig. 2a; p ≤ 0.001 for all genes) and proliferating HSPCs 12 hours after 2Gy IR treatment. Results are expressed as log2 fold expression compared to levels measured in the same unirradiated cells cultured for 12 hours *in vitro* (n = 3; ***p ≤ 0.001, **p ≤ 0.01, *p ≤ 0.05 [irradiated *vs*. unirradiated cells]. **C**, Immunofluorescence microscopy of γH2AX IRIF in unirradiated and 2Gy-irradiated resting and proliferating HSPCs. The percentage of positive cells (≥ 6 γH2AX positive foci) is shown over 24 hours (n = 3 to 5; scale bar = 10 μm).

A

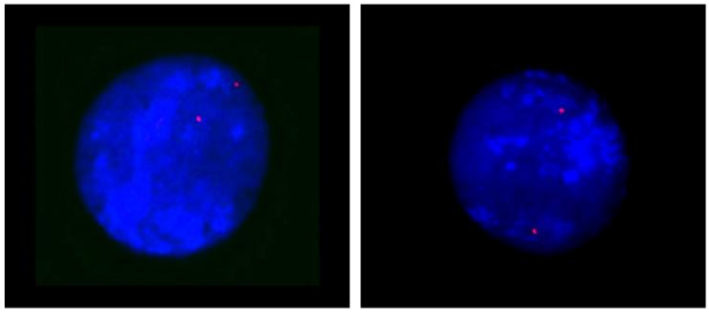

B

Treatment		1*	2	3	4	>4	# cells analyzed
Exp. I							
HSPC-derived cells	0Gy	3	190	1	7	0	201
	2Gy	4	192	1	1	2	200
Exp. II							
HSPC-derived cells	0Gy	14	180	5	2	0	200
	2Gy	8	196	9	5	0	218

Figure S6, FISH analysis of a mouse common fragile site region, related to Figure 7. A, Example of hybridization with a probe for the mouse *Fhit* locus common fragile site. FISH analyses were performed on the progeny of unirradiated or 2Gy-irradiated resting HSPCs expanded in culture for 4 days. Interphase nuclei were counterstained with DAPI. **B**, Quantification of the distribution of *Fhit* FISH signals in two independent experiments.

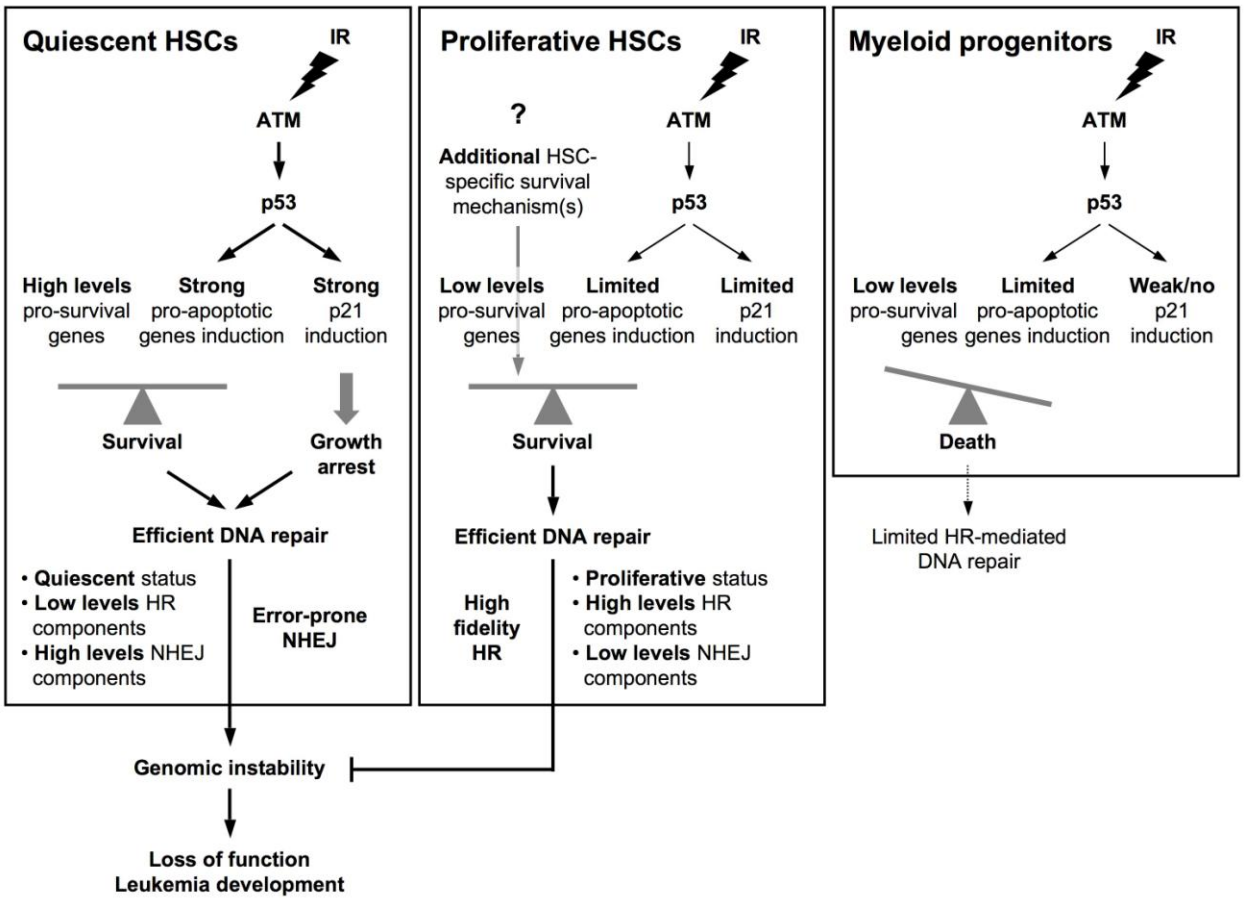

Figure S7, Model describing the molecular mechanism and mutagenic consequences of DNA repair in HSCs and myeloid progenitors, related to all Figures. Long-lived HSCs have unique cell-intrinsic mechanisms ensuring their survival in response to genotoxic stress such as ionizing radiation (IR) that are independent of their cell cycle status. Quiescent HSCs have enhanced pro-survival gene expression and robust p53-mediated induction of *p21* expression, which together buffer the strong accompanying induction of *bcl2*-family pro-apoptotic genes leading essentially to growth arrest, survival and DNA repair. Proliferative HSCs, like myeloid progenitors, have decreased pro-survival gene expression and attenuated p53-mediated DNA damage response leading to limited induction of both *p21* and *bcl2*-family pro-apoptotic genes. As a consequence myeloid progenitors predominantly die in response to IR treatment, while proliferating HSCs engages additional, still unknown, protective mechanism(s) that ensure their survival. Quiescent HSCs are restricted to using the error prone nonhomologous end-joining (NHEJ) mechanism to repair DNA damage due to their cell cycle status and molecular wiring of their DNA repair machinery, which renders them susceptible to genomic instability associated with misrepaired DNA. In contrast, proliferating HSCs, like the few surviving MPs, undergo DNA repair using the high fidelity homologous recombination (HR) mechanism and have a significantly decreased risk of acquiring mutation(s). Our results suggest that quiescent HSCs (either normal or leukemic) are intrinsically vulnerable to mutagenesis and represent an important source for leukemia development and bone marrow failure.

Table S1, DNA repair following irradiation *in vitro*, related to Figure 3.

	Average cell #/field	Normalized COMET tail DNA content				
		0	**1**	**2**	**3**	**4**
2Gy-irradiated HSPC						
2h post-IR	12.5 ± 1.6	3.3 ± 3.0	1.4 ± 0.4	0.8 ± 0.1	3.5 ± 0.4	3.6 ± 1.3
24h post-IR	11.8 ± 1.9	3.6 ± 1.6	2.0 ± 1.7	3.4 ± 1.1	1.4 ± 0.1	1.4 ± 0.4
p value				*p ≤ 0.05*	*p ≤0.001*	*p ≤ 0.05*
2Gy-irradiated CMP						
2h post-IR	10.4 ± 0.6	1.7 ± 1.0	0.7 ± 0.6	2.7 ± 1.2	2.2 ± 0.9	3.2 ± 2.4
24h post-IR	6.6 ± 1.1	2.1 ± 0.4	0.6 ± 0.7	0.4 ± 0.4	1.6 ± 0.4	1.9 ± 0.9
p value	*p ≤ 0.01*			*p ≤ 0.05*		
2Gy-irradiated GMP						
2h post-IR	11.2 ± 0.8	4.0 ± 1.3	0.7 ± 0.4	0.9 ± 0.7	1.1 ± 0.8	4.5 ± 0.7
24h post-IR	4.5 ± 1.6	2.1 ± 0.2	0.2 ± 0.4	0.6 ± 0.9	0.8 ± 0.4	0.8 ± 0.5
p value	*p ≤ 0.01*					*p ≤ 0.01*

Results of alkaline COMET assays performed on HSPCs, CMPs and GMPs 2 hours and 24 hours after exposure to 2Gy irradiation. Scoring, normalization for the numbers of visual fields counted and calculation of COMET tail DNA content (arbitrary units) was performed as described in the detailed Experimental Procedures section. Results are expressed as average ± SD (n = 3 independent experiments) and *p* values are indicated when differences are considered to be statistically significant.

Table S2, Genetic rearrangements following irradiation *in vitro,* related to Figure 7.

Resting HSPC (0Gy)		
Un.1:	# cells analyzed:	20
	# aberrations:	0
	% of cells with aberrations:	0%
	Aberrations:	None
	Karyotype:	40,XX[20]
Un.2:	# cells analyzed:	20
	# aberrations:	0
	% of cells with aberrations:	0%
	Aberrations:	None
	Karyotype*:	40,XX[12]/40,XY[8]
Resting HSPC (2Gy)		
Rest.1:	# cells analyzed:	20
	# aberrations:	7
	% of cells with aberrations:	30%
	Aberrations:	Reciprocal translocations (3), interstitial deletions (2), chromosome gaps/breaks (2)
	Karyotype:	40,XX[14]/40,XX,t(2;9)(C2;E3)[1]/39,X,-X,t(1;17)(H3;A2)[1]/40,XX,del(6)(B3D)[1]/40,X,del(X)(A2D)[1]/40,X,t(X;4)(F1;B2)[1]/39,XX,chrg(2)(F3),chrg(3)(F3)[1]
Rest.2:	# cells analyzed:	20
	# aberrations:	4
	% of cells with aberrations:	25%
	Aberrations:	Interstitial deletions (1), dicentrics (1) and ring (1) chromosomes, acentric fragments (4)
	Karyotype:	40,XX[15]/40,XX,del(6)(A3G2)[2]/39,XX,dic(10;18)(A2;A2)[1]/48,X,r(X)(A?1?D),+r(X)(A?1?D)x9,del(6)(A3G2),-9[1]/80,XXXX,del(6)(A3G2)x2, +4ace[1]
Rest.3:	# cells analyzed:	20
	# aberrations:	10
	% of cells with aberrations:	35%§
	Aberrations:	Reciprocal translocations (2), interstitial deletions (3), chromosome gaps/breaks (4), acentric fragment (2)
	Karyotype:	40,XX[13]/80,XXXX,chrb(1)(D)[1]/40,XX,chtb(12)(C2),t(17;18)(B;E1)[1]/40,XX,t(3;11)(H3;A4),del(6)(C2G2)[1]/40,XX,+der(11)(E1E2)x2,-15,+19[1]/44,XX,+X,+8,+13,+17[1]/40,XX,del(6)(A1D),der(9)chrb(9)(D)del(9)(A2D)[1]/40,XX,chrg(1)(E3)[1]
Rest.4:	# cells analyzed:	20
	# aberrations:	7

	% of cells with aberrations:	35%
	Aberrations:	Complex four-break rearrangement (2), interstitial deletion (2), reciprocal translocations (2), unbalanced translocations (1)
	Karyotype*:	40,XX[9]/40,XY[4]/80,XXXX[1]/40,XY,t(12;16)(12;15)(D1;B3;E;E)[1]/40,XX,t(2;16)(A2;C1)[1]/40,XY, t(10;18)(C1;E1)[1]/36,XY,-1,-5,-6,-8,t(9;10)(10;6)(D;A1;C3;B1)[1]40,XX,del(19)(BD1)[1]/40,X,t(X;8) (B;B2)[1]
Proliferating HSPC (2Gy)		
Mob1:	# cells analyzed:	21
	# aberrations:	4
	% of cells with aberrations:	23.8%
	Aberrations:	Reciprocal translocations (1), deletions (1), chromosome gaps/breaks (2)
	Karyotype:	40,XX[16]/40,XX,t(1;4)(D;D3)[1]/40,XX,del(6)(A2D)[1]/41,XX,+17[1]/40,XX,chrb(5)(D)[1]/40,XX,chrb(2)(F3)[1]
Mob2:	# cells analyzed:	14
	# aberrations:	2
	% of cells with aberrations:	7.1%
	Aberrations:	Interstitial deletions (1), unbalanced translocations (1)
	Karyotype:	40,XX[13]/40,X,del(X)(A2F3),der(19)t(8;19)(A4;D1)[1]
24h preC:	# cells analyzed:	20
	# aberrations:	3
	% of cells with aberrations:	5%
	Aberrations:	Interstitial deletions (2), unbalanced translocations (1)
	Karyotype:	40,XY[19]/41,XY,+3,del(3)(BH4),der(3)del(3)(A1A2)t(3;3)(A1;F3)[1]

SKY cytogenetic analyses were performed on the progeny of 2Gy-irradiated resting HSPCs (n = 4) or proliferating HSPCs (n = 3; two mobilized HSPCs and one 24h pre-cultured HSPCs) expanded in culture for 4 and 5 days, respectively. *A mixture of male and female mice were used to isolate HSPCs. §Cells with numerical abnormalities only are not included in the percent of cells with aberrations.

Table S3, Genetic rearrangements persisting *in vivo*, related to Figure 7.

Unirradiated HSPCs		
Cohort U1	# cells analyzed:	20
	# aberrations:	1
	% of cells with aberrations:	5%
	Aberrations:	Acentric fragment (1)
	Karyotype*:	40,XX[10]/40,XY[9]/40,XY,+ace[1]
Cohort U2	# cells analyzed:	20
	# aberrations:	0
	% of cells with aberrations:	0%
	Aberrations:	none
	Karyotype*:	40,XY[22]/40,XX[1]
2Gy-irradiated HSPCs		
Cohort I1:	# cells analyzed:	20
	# aberrations:	0
	% of cells with aberrations:	0%§
	Aberrations:	None
	Karyotype*:	40,XX[3]/40,XY[16]/35,X,-X or -Y,-5,-7,-13, -19[1]
Cohort I2:	# cells analyzed:	20
	# aberrations:	1
	% of cells with aberrations:	55%
	Aberrations:	Balanced translocation
	Karyotype*:	40,XX[3]/40,XY[6]/40,XY,t(16;17)(C1;E4)[11]
Cohort I3:	# cells analyzed:	20
	# aberrations:	5
	% of cells with aberrations:	25%
	Aberrations:	Balanced translocation (1), chromosome gaps/breaks (4)
	Karyotype:	40,XY[15]/40,XY,t(9;18)(F1;E1)[1]/40,XY, chtb(12)(F1)[1]/40,XY,chrg(5)(D)[1]/40,XY, chrg(10)(C1)[1]/40,XY,chtb(3)(F1)[1]
Cohort I4:	# cells analyzed:	20
	# aberrations:	4
	% of cells with aberrations:	20%
	Aberrations:	Balanced translocation (1), inversion (1), chromosome gaps/breaks (2)
	Karyotype:	40,XY[17]/40,XY,inv(1)(A1C2)[1]/40,XY,chtb(1)(B),t(2;10)(H3;C1)[1]/40,XY,chtb(2)(B)[1]

Donor-derived ($CD45.1^+$) MPs ($Lin^-/c\text{-}Kit^+/Sca\text{-}1^-$) were isolated from mice reconstituted with 2Gy-irradiated HSPCs 4 months after transplantation. SKY cytogenetic analyses were performed on the progeny of these cells expanded overnight in culture. *A mixture of male and

female mice were used to isolate donor HSPCs. [§]Cells with random loss of chromosome are not included in the percent of cells with aberrations.

SUPPLEMENTARY EXPERIMENTAL PROCEDURES

Mice.

C57Bl/6-CD45.1 and C57Bl/6-CD45.2 mice were used as donor (4-8 week old) for most of the cell isolation and as recipient (8-12 week old) for cell transplantation procedures. *Atm*$^{-/-}$ mice (129/sv) were purchased from the Jackson Laboratory and both transgenic H2k-*bcl2* (C57Bl/6) and *Trp53*$^{-/-}$ (FVB/N) mice have been described (Domen et al., 2000; Liu et al., 2009). Cyclophosphamide/G-CSF mobilization of HSCs was performed as described (Morrison et al. 1997). Transplantations were performed by retro-orbital injection of purified cells. Recipient mice were either sub-lethally (9.5Gy) or lethally irradiated (11Gy), both delivered in split dose 3 hours apart, and given antibiotic-containing water for at least 6 weeks post-irradiation. Peripheral blood was obtained from retro-orbital bleeding and collected in 4 ml of ACK (150 mM NH_4Cl/10 mM $KHCO_3$) containing 10 mM EDTA for flow cytometry analysis. Donor and recipient cells were distinguished by expression of GFP or different allelic forms of CD45 (CD45.1 vs. CD45.2). All animal experiments were performed in accordance with UCSF Institutional Animal Care and Use Committee approved protocols.

Flow cytometry.

Staining and enrichment procedures for HSPC, CMP, and GMP cell sorting and analysis were performed as previously described (Passegué et al., 2005; Santaguida et al., 2009). For regular isolation, c-Kit-enriched bone marrow cells were stained with unconjugated rat lineage (B220, CD3, CD4, CD5, CD8, Ter119, Mac-1, Gr-1) antibodies/goat anti-rat-PE-TxR and directly conjugated c-Kit-APC, Sca-1-PB, Flk2-bio/streptavidin-Cy7PE, CD34-FITC and FcγR-PE antibodies. For staining of purified cells with CFSE or FITC-conjugated antibodies (CC3, BrdU), c-Kit-enriched bone marrow cells were stained with unconjugated rat lineage/goat anti-rat-PE-TxR, c-Kit-cy7APC, Sca-1-PB, Flk2-PE, CD34-bio/streptavidin-Cy7PE and FcγR-cy5.5PE antibodies. Cells were finally resuspended in Hank's buffered saline solution (HBSS) with 2% heat-inactivated fetal bovine serum (FBS) containing 1μg/ml propidium iodide (PI) for dead cell exclusion, and sorted or analyzed on a FACS AriaII or LSRII (Becton Dickinson), respectively. Each population was double sorted to ensure maximum purity and irradiated as needed using a ^{137}Cs source (600ci^{137}Cs; J.L Shepherd & Associates Radiation Machinery M38-1 S.N. 1098).

Cell cultures.

Both methylcellulose and liquid cultures were supplemented with SCF (25 ng/ml), Flt3-L (25 ng/ml), IL-11 (25 ng/ml), IL-3 (10 ng/ml), Tpo (25 ng/ml), Epo (4 U/ml) and GM-CSF (10 ng/ml) (Peprotech). For methylcellulose assays, cells (0-2Gy/4-10Gy: 100/500 HSPCs and CMPs; 250/1000 GMPs) were plated in Iscove's modified Dulbecco's media (IMDM) based methylcellulose (StemCell Technology M3231) and colonies were counted on day 7 using duplicate plates per condition. For growth expansion in liquid culture, 500 cells were plated per well of a 96-well plate in 200μl IMDM containing 5% FBS (StemCell Technology), 1x penicillin/streptomycin, 0.1mM non-essential amino acids, 1mM sodium-pyruvate, 2mM Gluta-Max-1, 50μM 2-mercaptoethanol. Medium was replenished and cells were expanded as needed to maintain optimal growth. Cells were counted on days 2, 4, 6 and 8 by trypan blue exclusion using triplicate wells per condition and time point. Other cell culture experiments were started with various numbers of purified (± irradiation) cells (5,000-40,000).

Apoptosis and proliferation assays.

Apoptosis levels were measured by flow cytometry using intracellular staining for FITC-conjugated cleaved caspase 3 according to the manufacturer's instructions (Becton Dickinson). For CFSE dilution assays, purified cells were washed once with PBS, incubated for 5 min at RT with 5 μM CSFE (Molecular Probes/Invitrogen) in PBS, immediately quenched with an equal volume of FBS, washed twice with complete IMDM media, eventually irradiated and then cultured as needed before flow cytometry analysis. For intracellular BrdU staining, purified cells were incubated for 1 hour with 60μM BrdU (Sigma), fixed in PBS/4% PFA for 20 min at RT, washed twice in PBS/50mM NH_4Cl, permeabilized in PBS/0.2% Triton-X100 for 5 min and washed in low PB (0.2x PBS, 3% BSA) buffer. Cells were then incubated with 50U DNAseI in low PB buffer containing 5 mM $MgCl_2$/2 mM $CaCl_2$ for 30 min at RT min, washed once with low PB buffer, incubated for 30 min with FITC-conjugated anti-BrdU antibody (Pharmingen), washed once and resuspended in low PB buffer without PI for flow cytometry analysis. 7AAD/Pyronin Y staining and p53 intracellular staining were performed as previously described (Santaguida et al., 2009).

Quantitative RT-PCR.

Total RNA was isolated using TRIzol or TRIzol-LS (Invitrogen) from equivalent numbers of purified cells (20,000 to 50,000 aliquots), digested with DNase I and used for random hexamer-based reverse-transcription according to the manufacturer's instructions (SuperScript III™ kit, Invitrogen). QRT-PCR primers were designed using Primer Express software (Applied Biosystems) and are listed in the table below. All reactions were performed in an ABI-7300 sequence detection system using SYBR® Green PCR Core reagents (Applied Biosystems) and the cDNA equivalent of 200 cells as previously described (Santaguida et al., 2009). Each measurement was performed in triplicate and expression levels of β-actin were used to normalize the amount of the investigated transcript.

Western blot.

Purified 35,000 - 70,000 cell aliquots were pelleted, washed once with PBS, lysed in RIPA buffer (50mM Tris-HCl pH7.4, 150mM NaCl, 1% NP40, 0.5% Na-deoxycholate, 0.1% SDS, 1mM EDTA, 1mM Na_3VO_4, 1mM NaF and complete protease inhibitor cocktail [Roche Diagnostics]) for 30 min at 4°C, cleared of debris by centrifugation, boiled in SDS sample buffer and entirely deposited in one lane of a 12% SDS- polyacrylamide gel as previously described (Picariello et al., 2006). Briefly, samples (≤ 5μg total protein) were resolved by electrophoresis, transferred to nitrocellulose membranes, blocked for 1 hour at 4°C in blocking buffer (LI-COR Biosciences), incubated overnight at 4°C in blocking buffer/0.1% Tween 20 containing primary antibodies (anti-Mcl-1 [600-401-394, Rockland], rabbit polyclonal anti-Bid [gift from Dr. G. Shore, McGill University], rabbit polyclonal phospho-p53 (Ser15) [9284, Cell Signaling], anti-Actin [A2066, Sigma]), washed once in PBS/0.1% Tween 20, incubated for 1 hour at 4°C in blocking buffer/0.1% Tween 20 containing the appropriate IRDye conjugated secondary antibody (goat-anti-mouse IRDye 680 [926-32220]; goat-anti-rabbit IRDye 800CW dye [926-32211]; LI-COR Biosciences) washed 3 times in PBS/0.1% Tween 20 and visualized using an Odyssey Infrared Imager (LI-COR Biosciences).

Immunofluorescence microscopy.

Purified cells (± irradiation) grown in 5,000 (HSPCs) or 30,000 (MPs) cell aliquots were cytospun onto poly-lysine coated slides (Sigma) for 2 min at 200 rpm, fixed in PBS/4% PFA for 10 min at RT, permeabilized in PBS/0.15% Triton-X100 for 2 min at RT, blocked 1 hour at RT to overnight at 4°C in PBS/1%BSA and stained as previously described (Dodson et al., 2004). Briefly, cells were incubated for 1 hour at 37°C in PBS/1%BSA containing primary antibodies (anti-phospho-H2AX S139 [JBW301, Millipore], 53BP1 [NB100-904, Novus Biologicals], Rad51 [sc-8349, Santa Cruz]), washed twice in PBS, incubated for 1 hour at 37°C in PBS/1%BSA containing the appropriate Alexa-conjugated secondary antibody (goat-anti-mouse A488 [A11001]; goat-anti-rabbit A594 [A11037]; Invitrogen) washed twice in PBS and then mounted in VectaShield (Vector Laboratories) containing 1µg/ml DAPI (Sigma). Microscopy imaging was performed using an Olympus BX-51 microscope (100x objective, NA 1.35 lens) driven by the OpenLab software. Deconvolved (nearest neighbor DCI) images were saved as Photoshop CS files. Cells were scored as positive or negative based on the number of foci observed by eye. All scoring was done blind and 30-50 cells were counted per time point in each experiment.

Alkaline COMET Assay.

Purified cells (± irradiation) grown in 10,000 (HSPCs) or 30,000 (CMPs and GMPs) cell aliquots were washed once in mincing buffer (Mg^{2+}/Ca^{2+}-free HBSS, 20mM EDTA, 10% DMSO, pH7-7.5), resuspended in 100µl molten (42°C) 0.5% low melting point agarose (LMP, Promega) in PBS, and rapidly spread on slides (Superfrost Plus Micro, Fisher) coated in advance with normal melting point agarose (Sigma) without prior washing or dry cleaning. Slides were then coverslipped, allowed to solidify for at least 10 min at 4°C and processed as previously described (Klaude et al., 1996). Briefly, upon coverslip removal, slides were incubated from 4 hours to overnight at 4°C in lysis buffer (2.5M NaCl, 100 mM EDTA, 10 mM Tris/pH10 with freshly added 10% DMSO and 1% Triton-X100), rinsed once with neutralization buffer (0.4M Tris-pH7.5), incubated for 25 min on wet ice in fresh electrophoresis buffer (0.3M NaOH, 1M EDTA, pH 13) for unwinding of DNA and run for 30 min at 0.5 V/cm and 300 mA in the same buffer. After electrophoresis, slides were washed twice for 5 min in neutralization buffer, dehydrated at RT in absolute ethanol, stained with 100 µl SyberGold (Invitrogen) and coverslipped. Observations were made at a magnification of 200X using a Nikon E800 epifluorescence microscope with FITC barrier filter. Cells were analyzed and scored by visual classification as no statistical difference between visual and automated tail moment quantification has been demonstrated (Kobayashi et al., 1995; Jalaszynski et al., 1997). For each condition, ~ 500 cells were counted and the number of visual fields required to count that number recorded. DNA damage severity was assessed on a 0 (un-damaged) to 4 (very damaged/dead) progressive scale. The COMET tail DNA content score represents the number of cells counted for each 0-4 categories. Normalization between conditions was done by dividing the COMET tail DNA content scored for each category by the total number of visual fields counted. The percentage tail DNA (expressed in arbitrary units) was calculated based on the following equation adapted from[47]: % tail DNA = (0 x n0 + 1x n1 + 2 x n2 + 3 x n3 + 4 x n4) / (En x 4), where n0-n4 represent the numbers of cells counted in 0-4 categories and En the total number of scored cells.

NHEJ activity assay.

C-Kit-enriched bone marrow cells (± irradiation) were pre-cultured for 12 hours in liquid media (full cytokine cocktail without Flt3-L) in 3-6x10^6 cell aliquots and electroporated with 2µg of BamH1-digested pcDNA-eGFP plasmid (which cleaves between the promoter and the eGFP ORF) and 2µg pcDNA-Tomato plasmid using the Amaxa mouse macrophage nucleofactor kit following the manufacturer's protocol (Lonza, Amaxa Inc, VPA-1009). Cells were then incubated for another 24 hours in liquid media (full cytokine cocktail without Flt3-L) and labeled with cell surface markers to determine the percentage of GFP expression in transfected Tomato$^+$ HSPCs, CMPs and GMPs by flow cytometry.

Cytogenetic analysis.

Purified cells (± irradiation) were grown for 3 days (MPs, 100,000 to 300,000 cell aliquots) or 4 days (HSPCs: 50,000 to 100,000 cell aliquots), treated for 4 hours with 0.01 µg/ml Colcemid™ (Invitrogen), collected in eppendorf tubes and washed once with PBS. Cells were incubated for 8 min at 37°C in 0.075M KCl and then fixed in 3:1 volume absolute methanol:glacial acetic acid. Spectral karyotyping analysis (SKY) was performed as described (Le Beau et al., 2002). At least 20 metaphase cells were analyzed per case. A labeled BAC probe (9J14, 219 kb) containing the mouse common fragile site sequences within the *Fhit* gene (MMU 14A2) was prepared by direct labeling with Spectrum Orange™-labeled nucleotides (Abbott Molecular Diagnostics). Fluorescence in situ hybridization (FISH) was performed as described (Le Beau et al., 1996). Cells were counterstained with DAPI, and ~ 200 interphase nuclei were scored for each sample.

Statistics.

All the data are expressed as mean ± standard deviation (error bar) except when indicated. P values were generated using unpaired Student's *t*-test and considered significant when ≤ 0.05. N indicates the numbers of independent experiments performed.

SUPPLEMENTAL REFERENCES

Jalaszynski, P., Kujawaski, M., Czub-Swierczek, M., Markawaska, J. and Szyfter, K. (1997). Bleomycin induced DNA damage and its removal in lymphocytes of breast cancer patients studied by comet assay. Mutat Res *385*, 223-233.

Kobayashi, H., Sugiuama, C. Morikawa, Y., Hayashi, M. & Sofuni, T. A comparison between manual microscopic analysis and computerized image analysis in the single cell gel electrophoresis assay MMS. *Communic* **3**, 103-115 (1995).

Le Beau, M.M. *et al*. (1996). Cytogenetic and molecular delineation of a region of chromosome 7 commonly deleted in malignant myeloid diseases. Blood *88*, 1930-1935.

Picariello, L., Carbonell Sala, S., Martineti, V., Gozzini, A., Aragona, P., Tognarini, I., Paglierani, M., Nesi, G., Brandi, M.L., and Tonelli, F. (2006). A comparison of methods for the analysis of low abundance proteins in desmoid tumor cells. Anal Biochem *354*, 205-212.

QRT-PCR Primer Table.

Gene	Forward (5' to 3')	Reverse (5' to 3')	Accession	Ct range
A1	ccctggctgagcactacctt	ctgcatgcttggcttgga	NM_009742	31.3 ± 1.3
Bak	aatggcatctggacaaggac	gttcctgctggtggaggtaa	NM_007523.1	21.9 ± 1.2
Bax	tggagctgcagaggatgattg	agctgccacccggaaga	NM_007527	25.1 ± 0.9
Bcl2	tgggatgcctttgtggaact	acagccaggagaaatcaaacag	NM_009741	24.3 ± 0.8
Bcl-xl	ggctgggacacttttgtggat	gcgctcctggcctttcc	NM_009743	26.4 ± 0.4
Bid	gaagacgagctgcagacagatg	aatctggctctattcttccttggtt	NM_007544.3	27.8 ± 1.9
Bim	ttggagctctgcggtcctt	cagcggaggtggtgtgaat	NM_009754	27.6 ± 0.4
Ku70	ggagtcaagcaagctggaaga	agaactcgctttttggtctcctt	NM_010247.2	27.1 ± 0.3
Ku80	gacttgcggcaatacatgttttc	aagctcatggaatcaatcagatca	NM_009533	27.7 ± 0.9
Mcl1	ccctcccccatcctaatcag	agtaacaatggaaagcatgccaat	NM_008562	26.4 ± 0.5
Noxa	ggagtgcaccggacataact	ttgagcacactcgtccttca	NM_021451.1	28.4 ± 0.8
Prkdc	gcccatgagcttaggtttcaat	ctaagagctttcagcaggttcaca	NM_011159.2	27.2 ± 0.4
Puma	gcggcggagacaagaaga	agtcccatgaagagattgtacatgac	NM_133234	28.8 ± 0.4
p21	ttccgcacaggagcaaagt	cggcgcaactgctcact	NM_007669	26.2 ± 0.8
Rad51	aagttttggtccacagcctattt	cggtgcataagcaacagcc	NM_011234.4	28.0 ± 1.1
Rad54	ccaggtccaggagtgtttcc	ggccggttgagtagctgagt	NM_009015.3	26.9 ± 1.1
Rpa.a1	acatccgtcccatttctacagg	ctccctcgaccagggtgtt	NM_026653.1	27.7 ± 0.8
Smc6	ccgtgtgcttcatcctttcc	ccatatccatgtagacatcaaactca	NM_025695.4	27.9 ± 0.6
Trp53	aagatccgcgggcgtaa	catcctttaactctaaggcctcattc	NM_011640.1	22.8 ± 0.8
Xrcc2	ggaaaggcccacatgtgagt	ggatcgtttgtgacataggcatt	NM_020570.2	29.7 ± 1.0
Xrcc3	cctgaggagctgatcgagaaga	cggccgcgtgttcaat	NM_028875.2	28.6 ± 0.9
β-actin	gacggccaggtcatcactattg	aggaaggctggaaaagagcc	NM_007393	21.7 ± 0.3

The range of Ct values (± SD) obtained for each gene when performing qRT-PCR analysis with the cDNA equivalent of 200 cells (HSPCs, CMPs or GMPs) per reaction is indicated.